ELSEVIER

MHD-free convection from a vertical plate embedded in a thermally stratified porous medium with Hall effects

Ali J. Chamkha

Department of Mechanical and Industrial Engineering, Kuwait University, Safat, Kuwait

The problem of the free convection flow of an electrically conducting fluid along a vertical plate embedded in a thermally stratified porous medium in the presence of a uniform normal magnetic field is investigated. The basic equations comprising the balance laws of mass, linear momentum, and energy modified to include the porous medium Darcian and non-Darcian effects, the Hartmann and Hall effects of magnetohydrodynamics, and the thermal stratification of the porous medium are solved numerically using the finite difference method. Graphical results for the velocity, temperature, skin-friction, and the local Nusselt number profiles are illustrated and discussed for various physical parametric values. © *1997 by Elsevier Science Inc.*

Keywords: MHD flow, free convection, thermal stratification, porous media

1. Introduction

Buoyancy-induced flow along an isothermal vertical plate embedded in a porous medium is a fundamental problem in fluid and heat-transfer areas. This type of problem has received considerable attention recently due to possible applications in many industries involving heat exchanger design, petroleum production, filtration, chemical catalytic reactors, and nuclear waste repositories. Tien and Vafai[1] reported the extent of research on this topic and discussed the importance of the non-Darcian boundary and inertia effects that account for the presence of a solid boundary and moderate velocity flow in the porous medium. Recent work on free convection flow in thermally stratified porous media have been reported by several investigators (see, for instance, Bejan,[2] Nakayama and Koyama,[3] Takhar and Pop,[4] Singh and Tewari,[5] and Chen and Lin[6]. Similar research has been carried out on electrically conducting fluids in the presence of a magnetic field to study the effects of the magnetic field on flow and heat-transfer aspects (see, for example, Sparrow and Cess,[7] Gupta,[8] Singh and Cowling,[9] Riley,[10] Kuiken,[11] Wilks,[12] Wilks and Hunt,[13] Watanabe and Pop,[14] and Pop and Watanabe.[15] Among all these investigations only Pop and Watanabe[15] consider the effects of MHD Hall currents, which are important for ionized gas at high Hartmann numbers. In this paper ideas borrowed from the works of Singh and Tewari,[5] Chen and Lin,[6] and Pop and Watanabe[15] are incorporated into a model that describes the MHD-free convection boundary layer flow of an electrically conducting fluid along a vertical plate immersed in a thermally stratified fluid-saturated porous medium. The model accounts for Darcian and non-Darcian effects of the porous medium and the Hall effects of magnetohydrodynamics. It is assumed that the magnetic Reynolds number is small so that the induced magnetic field is neglected. The flow is assumed steady, laminar, and incompressible.

2. Governing equations

Consider a steady, laminar, incompressible, free convection boundary-layer flow along a vertical plate embedded in a thermally stratified fluid-saturated porous medium in the presence of a uniform normal magnetic field. The plate is maintained at a constant temperature T_w, and the ambient temperature or that of the stratified porous medium varies linearly with height. Let the x- and y-axes be parallel and normal to the plate, respectively, and let the z-axis be coincident with the leading edge of the plate. As mentioned before the Hall effects are assumed significant in this problem. The presence of these effects in the model gives rise to a force in the z-direction that induces a cross-flow in that direction (see Pop and Watanabe[15]). The governing equations for this investigation are based on the balance laws of mass, linear momentum, and energy modified to include the porous medium Darcian and non-Darcian effects with generalized Ohm's and

Address reprint requests to Dr. A. J. Chamkha at Kuwait University, Department of Mechanical Engineering, Safat 13060, Kuwait.

Received 9 October 1996; revised 9 June 1997; accepted 3 July 1997.

Appl. Math. Modelling 1997, 21:603–609, October

655 Avenue of the Americas, New York, NY 10010

0307-904X/97/$17.00
PII S0307-904X(97)00084-X

Maxwell's laws. With the usual boundary-layer and Boussinesq approximations the problem is governed by the following equations (see, for instance, Chen and Lin[6] and Pop and Watanabe[15])

$$\frac{\partial u}{\partial x}+\frac{\partial v}{\partial y}=0 \tag{1}$$

$$\frac{1}{\epsilon^2}\left(u\frac{\partial u}{\partial x}+v\frac{\partial u}{\partial y}\right)=g\beta(T-T_\infty(x))+\frac{\nu}{\epsilon}\frac{\partial^2 u}{\partial y^2}-\frac{\nu}{K}u-Cu^2-\frac{\sigma_0 B_0^2}{\rho(1+m^2)}(u+mw) \tag{2}$$

$$\frac{1}{\epsilon^2}\left(u\frac{\partial w}{\partial x}+v\frac{\partial w}{\partial y}\right)=\frac{\nu}{\epsilon}\frac{\partial^2 w}{\partial y^2}-\frac{\nu}{K}w-Cw^2-\frac{\sigma_0 B_0^2}{\rho(1+m^2)}(w-mu) \tag{3}$$

$$u\frac{\partial T}{\partial x}+v\frac{\partial T}{\partial y}=\alpha\frac{\partial^2 T}{\partial y^2} \tag{4}$$

where x and y are the distances parallel and normal to the plate, respectively. u, v, and w are the fluid velocity components in the x-, y-, and z-directions, respectively. T and T_∞ are the fluid and ambient temperatures, respectively. ρ and ν are the fluid density and kinematic viscosity, respectively. g and β are the acceleration due to gravity and the coefficient of volumetric thermal expansion, respectively. ϵ, K, C, and α are the porosity, permeability, inertia coefficient, and effective thermal diffusivity of the porous medium, respectively. σ_0, B_0, and m are the fluid electrical conductivity, magnetic induction, and the Hall parameter, respectively. It should be mentioned that the plate is assumed to be electrically nonconducting.

In the present study the ambient temperature is assumed to vary linearly with the vertical distance x as follows

$$T_\infty(x)=T_{\infty,x=0}+sx \tag{5}$$

where $T_{\infty,x=0}$ is the ambient temperature at the plate's leading edge and $s=dT_\infty(x)/dx>0$ is a stratification rate parameter. The increasing behavior of the ambient temperature with x is chosen to ensure stable stratification. It should be mentioned that the leading edge of the plate is at a temperature above that of the surrounding fluid at the same elevation. Therefore it must be presumed that the plate is of finite length (see Singh and Tewari[5]). The finite plate length is necessary because at the condition when the wall temperature T_w is equal to the ambient temperature $T_\infty(x)$, the plate starts to act as a cooler, which will result in a flow separation.

The boundary conditions suggested by the physics of the problem are

$$\begin{aligned}&u(0,y)=0,w(0,y)=0,T(0,y)=T_w\\&u(x,0)=0,v(x,0)=0,w(x,0)=0,T(x,0)=T_w\\&u(x,\infty)=0,w(x,\infty)=0,T(x,\infty)=T_\infty(x)\end{aligned} \tag{6}$$

It is convenient to make the governing equations and conditions dimensionless similar to Chen and Lin,[6] by using

$$\begin{aligned}&x=L\xi,\ y=LGr^{-1/4}\eta,\ u=\frac{\nu Gr^{1/2}}{L}F,\ v=\frac{\nu Gr^{1/4}}{L}G\\&w=\frac{\nu Gr^{1/2}}{L}H,\ \theta=\frac{T(x,y)-T_\infty(x)}{T_w-T_{\infty,x=0}}\\&Gr=\frac{g\beta(T_w-T_{\infty,x=0})L^3}{\nu^2},\ \Gamma=CL,\ \psi=\frac{K}{L^2}Gr^{1/2}\end{aligned} \tag{7}$$

where L is a characteristic plate length.

Substituting equation (7) into equation (1) through equation (6) and rearranging yield

$$\frac{\partial F}{\partial\xi}+\frac{\partial G}{\partial\eta}=0 \tag{8}$$

$$\frac{1}{\epsilon^2}\left(F\frac{\partial F}{\partial\xi}+G\frac{\partial F}{\partial\eta}\right)=\theta+\frac{1}{\epsilon}\frac{\partial^2 F}{\partial\eta^2}-\frac{1}{\psi}F-\Gamma F^2-\frac{M^2}{1+m^2}(F+mH) \tag{9}$$

$$\frac{1}{\epsilon^2}\left(F\frac{\partial H}{\partial\xi}+G\frac{\partial H}{\partial\eta}\right)=\frac{1}{\epsilon}\frac{\partial^2 H}{\partial\eta^2}-\frac{1}{\psi}H-\Gamma H^2-\frac{M^2}{1+m^2}(H-mF) \tag{10}$$

$$F\frac{\partial\theta}{\partial\xi}+SF+G\frac{\partial\theta}{\partial\eta}=\frac{1}{\mathrm{Pr}}\frac{\partial^2\theta}{\partial\eta^2} \tag{11}$$

$$\begin{aligned}&F(0,\eta)=0,H(0,\eta)=0,\theta(0,\eta)=1.0\\&F(\xi,0)=0,G(\xi,0)=0,H(\xi,0)=0,\\&\theta(\xi,0)=1-S\xi\\&F(\xi,\infty)=0,H(\xi,\infty)=0,\theta(\xi,\infty)=0\end{aligned} \tag{12}$$

where $M^2=\sigma_0 B_0^2 L^2/(\rho\nu Gr^{1/2})$, $S=Ls/(T_w-T_{\infty,x=0})$, and $\mathrm{Pr}=\nu/\alpha$ are the square of the Hartmann number, the dimensionless stratification rate parameter, and the Prandtl number, respectively.

Important physical flow and heat transfer parameters for this problem are the skin-friction coefficient and the

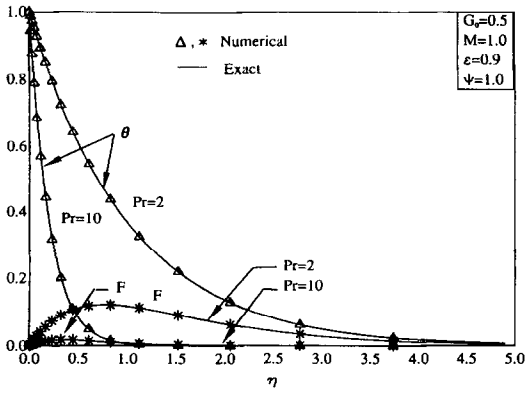

Figure 1. Comparison between exact and numerical solutions.

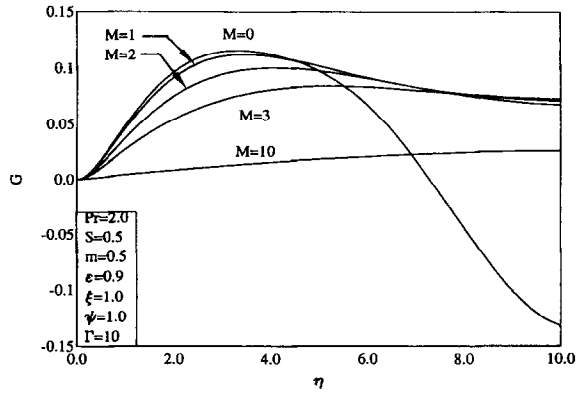

Figure 3. Normal velocity profiles for various Hartmann numbers.

local Nusselt number. These are defined in dimensionless form as

$$C_f = -Gr^{3/4}\frac{\partial F}{\partial \eta}(\xi,0),$$
$$N_x = -Gr^{1/4}\frac{\xi}{1+S\xi}\frac{\partial \theta}{\partial \eta}(\xi,0) \tag{13}$$

3. Analytical solutions

The governing equations presented in the previous section are nonlinear and exhibit no closed-form or similar solutions. In general such solutions can be very useful in validating computer routines of complicated problems and comparisons with experimental data. It is, therefore, of interest to reduce the governing equations of the present problem to a form that can be solved in closed form. A special case of the present problem that exhibits exact or closed-form solution is the problem of steady slow MHD-free convection flow along an infinite vertical porous plate embedded in a porous medium without stratification and for a low or moderate magnetic field strength. The slow flow and low magnetic field conditions indicate that both the medium inertia effects and the magnetic field Hall effects can be neglected. The resulting equations for this special problem can be written as

$$\epsilon\frac{d^2F}{d\eta^2} + G_0\frac{dF}{d\eta} - \epsilon^2\left(\frac{1}{\psi}+M^2\right)F + \epsilon^2\theta = 0 \tag{14}$$

$$\epsilon\frac{d^2H}{d\eta^2} + G_0\frac{dH}{d\eta} - \epsilon^2\left(\frac{1}{\psi}+M^2\right)H = 0 \tag{15}$$

$$\frac{d^2\theta}{d\eta^2} + G_0\,\mathrm{Pr}\frac{d\theta}{d\eta} = 0 \tag{16}$$

where $d(\ )/d\eta$ indicates ordinary differentiation with respect to η and $G_0 > 0$ is a constant suction velocity. Equations (14) through (16) subject to

$$F(0) = 0, H(0) = 0, \theta(0) = 1$$
$$F(\infty) = 0, H(\infty) = 0, \theta(\infty) = 0 \tag{17}$$

possess the following solutions

$$\theta = \exp(-G_0\,\mathrm{Pr}\,\eta), H = 0$$
$$F = A(\exp(-G_0\,\mathrm{Pr}\,\eta) - \exp(-\lambda\eta)) \tag{18}$$

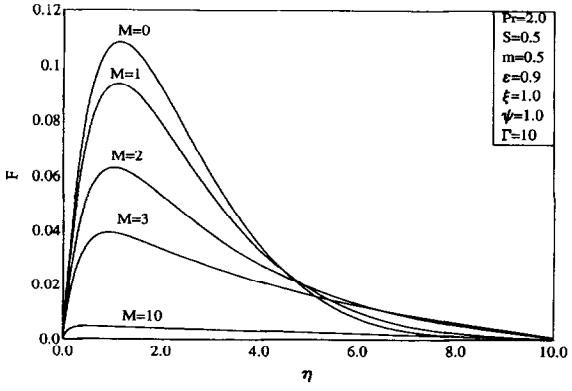

Figure 2. Tangential velocity profiles for various Hartmann numbers.

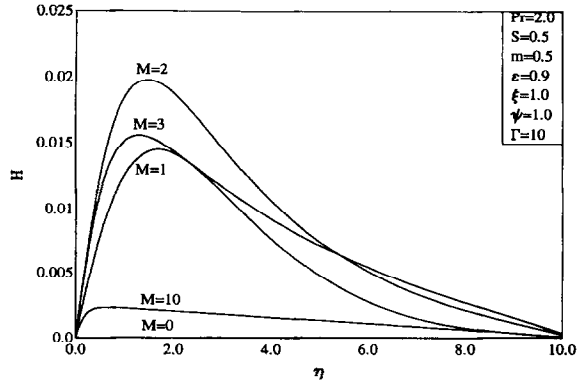

Figure 4. Lateral velocity profiles for various Hartmann numbers.

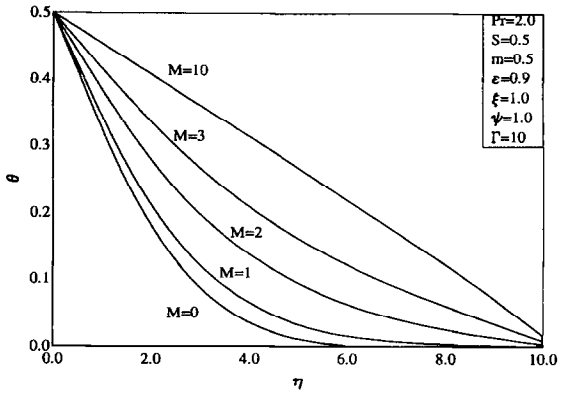

Figure 5. Temperature profiles for various Hartmann numbers.

where

$$\lambda = \frac{G_0 + \left(G_0^2 + 4\epsilon^3\left(\frac{1}{\psi} + M^2\right)\right)^{1/2}}{2\epsilon}$$
$$A = \frac{\epsilon^2}{G_0^2 \Pr(1 - \epsilon \Pr) + \epsilon^2\left(\frac{1}{\psi} + M^2\right)} \qquad (19)$$

The skin-friction coefficient and the Nusselt number for this special case take on the form

$$C_f = Gr^{3/4}A(G_0 \Pr - \lambda), \mathbf{N} = Gr^{1/4}G_0 \Pr \qquad (20)$$

As the suction parameter G_0 approaches zero the above solutions reduce to

$$\theta = 1, F = -A^* \exp(-\lambda^* \eta), C_f = -Gr^{3/4}A^*\lambda^*, \mathbf{N} = 0$$
$$\lambda^* = \left(\epsilon\left(\frac{1}{\psi} + M^2\right)\right)^{1/2}, A^* = \frac{1}{\left(\frac{1}{\psi} + M^2\right)} \qquad (21)$$

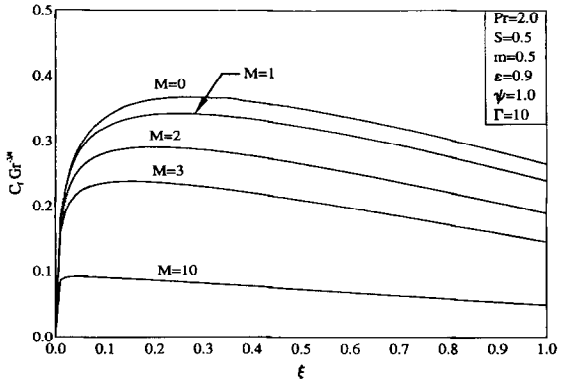

Figure 6. Skin friction coefficient for various Hartmann numbers.

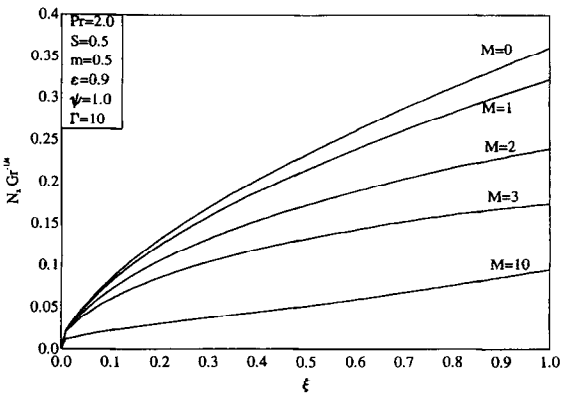

Figure 7. Local Nusselt number for various Hartmann numbers.

4. Numerical solutions

The complete form of equations (8) through (12) is solved numerically using an implicit, tridiagonal, iterative finite difference method similar to that discussed by Blottner[16] and Patankar.[17] All first-order partial derivatives with respect to ξ appearing in these equations are replaced by two-point backward difference formulas. Equations (9) through (11) are discretized by three-point central difference quotients while η differencing of equation (8) is done using the trapezoidal rule. The computational domain is divided up into 101 nodes in the ξ-direction and 196 nodes in the η-direction. Constant step sizes in the ξ-direction and variable step sizes in η-direction are employed with initial step sizes $\Delta\xi = 0.01$ and $\Delta\eta_1 = 0.001$. The growth factor for the η-direction employed in the present problem is 1.03. The number of nodes in both directions were chosen after much numerical experimentation was performed to assess grid independence. The problem is solved as an initial value problem with ξ playing the role of time. At each line of constant ξ linear tridiagonal algebraic equations are solved by the Thomas' algorithm (see, for instance, Blottner[16]). Iteration is employed to deal with the nonlinearities of the governing equations. A convergence criterion based on the difference of the current and the previous iterations was used.

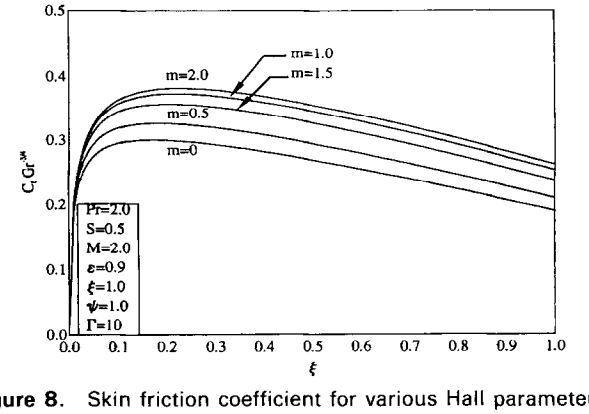

Figure 8. Skin friction coefficient for various Hall parameters.

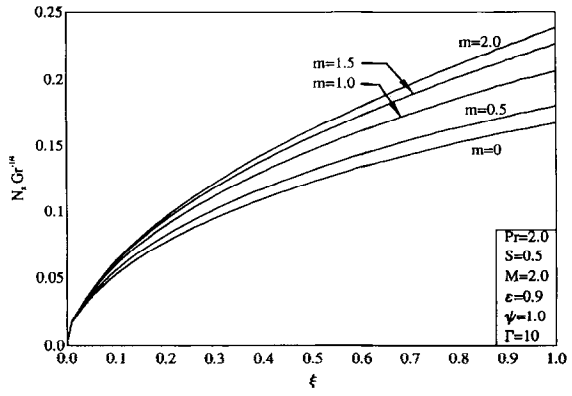

Figure 9. Local Nusselt number for various Hall parameters.

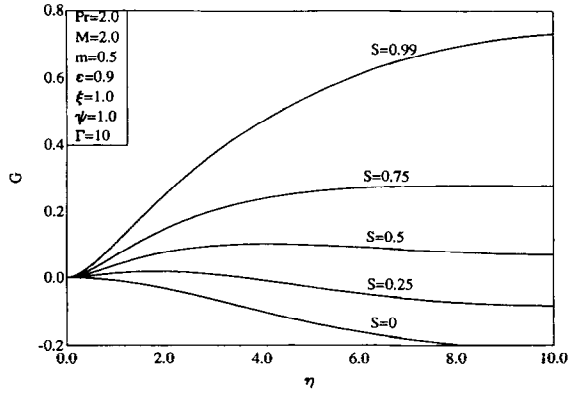

Figure 11. Normal velocity profiles for various stratification parameters.

Convergence was accomplished when this difference reached an acceptable limit. A value of 10^{-5} was employed in the present study.

The analytical solutions reported in the previous section were used as a check on the accuracy and effectiveness of the numerical procedure. For large values of ξ a steady-state-like condition is reached in which all gradients with respect to ξ vanish. This corresponds to the case of an infinite plate similar to that considered in the previous section. A comparison between the analytical results for the velocity and temperature reported above and their corresponding numerical results is given in *Figure 1*. As is evident from this figure the agreement between these results is excellent. This comparison lends confidence in the numerical solutions and shows that the numerical method is adequate for the solution of the present problem.

Figures 2 through *17* present fully numerical results for the velocity and temperature profiles as well as the skin-friction coefficient and the local Nusselt number for various parametric values. These figures are obtained to illustrate the relative influence of the Hartmann number, Hall parameter, stratification parameter, and the porous medium inertial parameter.

Figures 2 through *5* show typical profiles for the fluid tangential velocity F, normal velocity G, lateral velocity H, and temperature θ for different values of Hartmann number M, respectively. Increases in the values of M have a tendency to slow the motion of the fluid and make it warmer as it moves along the vertical plate causing F and G to decrease and θ to increase. These behaviors are clearly illustrated in *Figures 2, 3,* and *5*. In the absence of the magnetic field ($M = 0$) there is no lateral velocity ($H = 0$), and a reversal flow condition exists as shown in *Figure 3*. This is caused by a decrease in the thermal buoyancy that inhibited the flowing fluid coming from upstream. Thus the normal velocity G becomes negative in a small region far from the plate. However, as the flow resistance due to the presence of the magnetic field increases, the flow reversal condition diminishes (see Chen and Lin[6]). Also, as M becomes finite but relatively small, a cross-flow in the lateral direction is induced. In the limit as M becomes very large H becomes very small. This indicates that the lateral velocity increases and then decreases as M increases from relatively small to relatively large values. This is clearly depicted in *Figure 4*.

Figures 6 and *7* depict the variations of the skin-friction coefficient C_f and the local Nusselt number N along the plate for various values of the Hartmann number M, respectively. As M increases, the tangential velocity and temperature profiles decrease and increase, respectively, while their corresponding slopes at the plate's surface decrease. This causes both the skin-friction coefficient and the local Nusselt number to decrease. This is evident from the decreases in C_f and N_x as M increases in *Figures 6* and *7*, respectively.

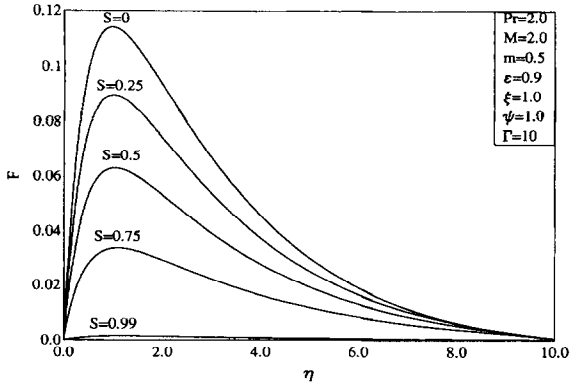

Figure 10. Tangential velocity profiles for various stratification parameters.

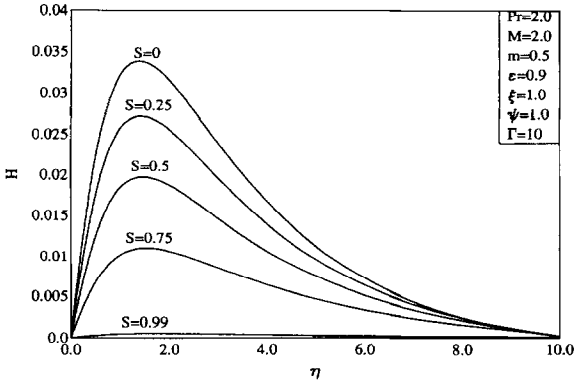

Figure 12. Lateral velocity profiles for various stratification parameters.

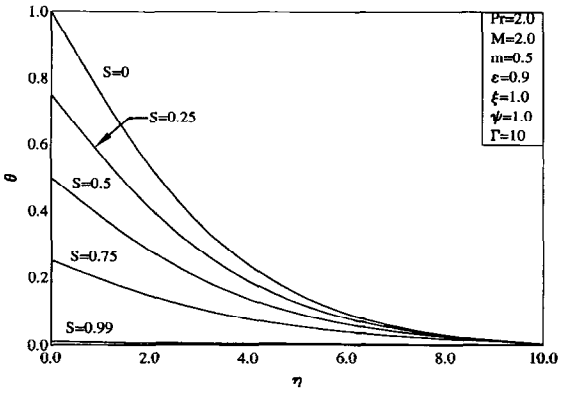

Figure 13. Temperature profiles for various stratification parameters.

Figures 8 and *9* are obtained by fixing the values of all the parameters (as shown in the figures) and by allowing the Hall parameter m to vary. Unlike the Hartmann number M increasing the values of m causes the fluid tangential and normal velocities to increase and its temperature to decrease at any point across the plate. However, since the lateral velocity vanishes both for $m = 0$ and as m becomes very large, it, therefore, increases and then decreases for the same reasons mentioned earlier for the effect of M. These behaviors are not shown here for brevity. Also increases in the values of m have a tendency to increase the frictional effects and to augment the heat transfer at the wall. This is reflected in the increases in the skin-friction coefficient and the local Nusselt number as m increases, shown in *Figures 8* and *9*, respectively.

Figures 10 through *15* depict the influence of the stratification parameter S on the velocity profiles F, G, and H, the temperature profiles θ, the skin-friction C_f, and the local Nusselt number N_x, respectively. As the stratification parameter increases the thermal buoyancy of the fluid decreases, as illustrated in *Figure 13*. This results in decreasing the fluid tangential and lateral velocities and increasing its normal velocity as is clearly shown in *Figures 10* through *12*. In addition the slope of the tangential velocity at the plate surface is decreased as S is increased, which yields a reduction in the values of C_f. From the

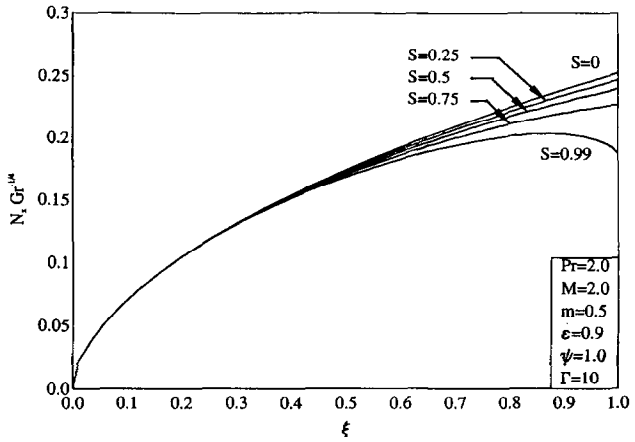

Figure 15. Local Nusselt number for various stratification parameters.

definition of N_x one expects it to decrease as S is increased, as is clearly shown in *Figure 15*. It should be noted that for small values of S ($S < 0.25$) a horizontal plume results, as demonstrated by Chen and Eichhorn.[18] This is reflected in the flow-reversal condition as G becomes negative for the small values of S observed in *Figure 11*.

Figures 16 and *17* present representative profiles for the skin-friction coefficient and the local Nusselt number for the various non-Darcian porous medium inertia parameter Γ, respectively. The medium inertia effects constitute resistance to flow. Thus as the inertia parameter Γ increases, the resistance to the flow increases, causing the fluid flow in the porous medium to slow down. This results in reducing the net velocity and, therefore, all its components as well as the wall friction. This is depicted in the decreases in C_f shown in *Figure 16* as Γ increases. Also increasing Γ has a tendency to warm up the fluid and to reduce the wall heat transfer as illustrated in the decreases in N_x shown in *Figure 17* as Γ increases.

The correctness of the numerical results was confirmed by direct comparisons with the closed-form solutions presented earlier for the steady state with and without wall suction (see *Figure 1*) and with the numerical results reported by Chen and Lin[6] for electrically nonconducting

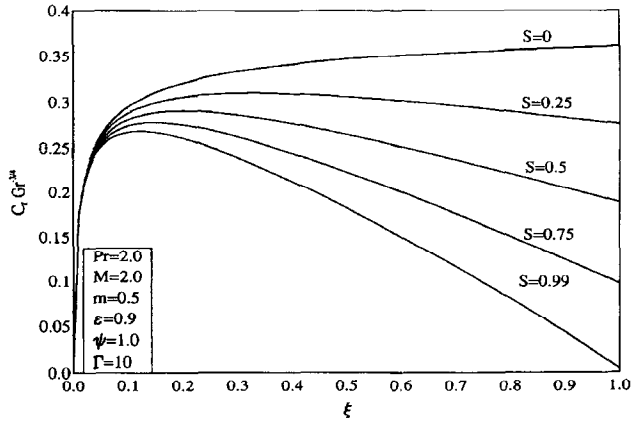

Figure 14. Skin friction coefficient for various stratification parameters.

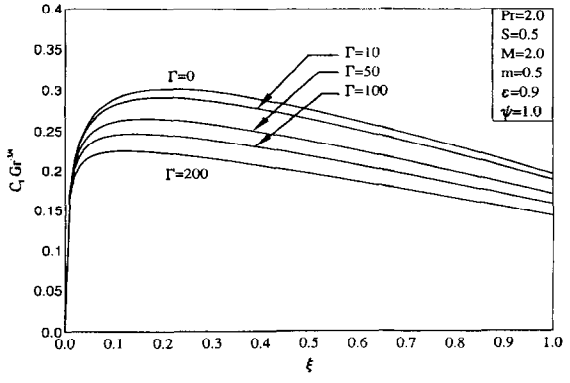

Figure 16. Skin friction coefficient for various medium inertial coefficients.

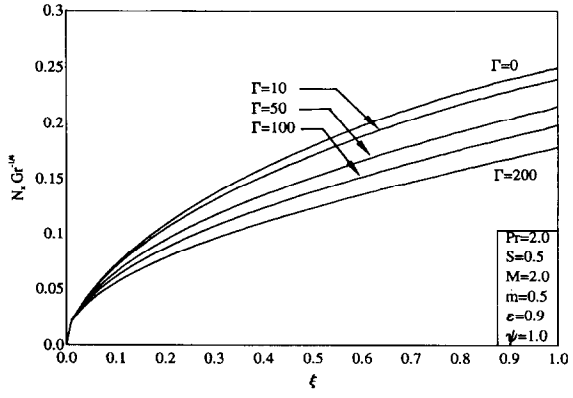

Figure 17. Local Nusselt number for various medium inertial coefficients.

fluids. Excellent agreement of results was obtained from these comparisons. It should be mentioned that the best comparisons can be accomplished when performed with experimental data. However this was not possible for the present problem due to the absence of such data at present.

5. Conclusion

The problem of free convection boundary-layer flow of an electrically conducting fluid along a vertical flat plate embedded in a thermally stratified porous medium in the presence of a uniform normal magnetic field was investigated. The governing continuum equations that comprised the balance laws of mass, linear momentum, and energy modified to include the porous medium Darcian and non-Darcian effects, the Hartmann and Hall effects of magnetohydrodynamics, and the thermal stratification of the porous medium were solved numerically using the finite difference method. Graphical results for the velocity, temperature, skin-friction, and the local Nusselt number profiles were presented and discussed for various physical parametric values. It was found that both the skin-friction coefficient and the local Nusselt number are decreased as the Hartmann number, the stratification parameter, or the medium inertia parameter is increased. Also increases in the Hall parameter caused increases in the skin-friction coefficient and the local Nusselt number. The numerical results were checked against closed-form solutions for the steady state and previously published numerical work. It is hoped that the present results will shed light on the various physical aspects of the problem and will serve as a stimulus for experimental work.

References

1. Tien, C. L. and Vafai, K. *Adv. Appl. Mech.* 1990, **27,** 225
2. Bejan, A. *Convective Heat Transfer.* Wiley, New York, 1984, pp. 367–371
3. Nakayama, A. and Koyama, H. *Appl. Sci. Res.* 1987, **46,** 309
4. Takhar, H. S. and Pop, I. *Mech. Res. Commun.* 1987, **14,** 81
5. Singh, P. and Tewari, K. *Int. J. Eng. Sci.* 1993, **31,** 1233
6. Chen, C. and Lin, C. *Int. J. Eng. Sci.* 1995, **33,** 131
7. Sparrow, E. M. and Cess, R. D. *Int. J. Heat Mass Transfer* 1961, **3,** 367
8. Gupta, A. S. *J. Appl. Math. Phys. (ZAMP)* 1963, **13,** 324
9. Singh, K. R. and Cowling, T. G. *Q. J. Mech. Appl. Math.* 1963, **16,** 1
10. Riley, N. *J. Fluid Mech.* 1964, **18,** 577
11. Kuiken, H. K. *J. Eng. Math.* 1971, **5,** 51
12. Wilks, G. *J. Appl. Math. Phys. (ZAMP)* 1976, **27,** 621
13. Wilks, G. and Hunt, R. *J. Appl. Math. Phys. (ZAMP)* 1984, **35,** 34
14. Watanabe, T. and Pop, I. *Int. Comm. Heat Mass Transfer* 1993, **20,** 871
15. Pop, I. and Watanabe, T. *Int. J. Eng. Sci.* 1994, **32,** 1903
16. Blottner, F. G. *AIAA J.* 1970, **8,** 193
17. Patankar, S. V. *Numerical Heat Transfer and Fluid Flow.* McGraw-Hill, New York, 1980
18. Chen, C. and Eichhorn, R. *ASME J. Heat Transfer* 1976, **98,** 446